Supplementary information for

Qualitative and quantitative analysis of accumulation and biodistribution of polystyrene nanoplastics in zebrafish (Danio rerio) via artificial freshwater

Théogène Habumugisha[a,b], Zixing Zhang[a], Jean Claude Ndayishimiye[a,b,c], François Nkinahamira[a,b,d,e,f], Constance Uwizewe[g], Eric Cyubahiro[a,b], Abdul Rehman[a,b], Changzhou Yan[a], Xian Zhang [a,*]

[a]*Key Lab of Urban Environment and Health, Institute of Urban Environment, Chinese Academy of Sciences, Xiamen 361021, P.R. China*
[b]*University of Chinese Academy of Sciences, Beijing 100049, P.R. China*
[c]*Faculty of Biology, Shenzhen MSU-BIT University, Shenzhen 518172, P.R. China*
[d]*Shenzhen Key Laboratory of Organic Pollution Prevention and Control, Environmental Science and Engineering Research Center, Harbin Institute of Technology (Shenzhen), Shenzhen 518055, P. R. China.*
[e]*State Key Laboratory of Urban Water Resource and Environment, Shenzhen Key Laboratory of Organic Pollution Prevention and Control, School of Civil and Environmental Engineering, Harbin Institute of Technology Shenzhen, Shenzhen 518055, P. R. China.*
[f]*International Joint Research Center for Persistent Toxic Substances, Harbin Institute of Technology Shenzhen, Shenzhen 518055, P. R. China.*
[g]*Key Laboratory of Physical Oceanography, Ocean University of China, Qingdao 266100, P.R. China.*

***Corresponding authors:**

Xian Zhang, Institute of Urban Environment, Chinese Academy of Sciences, Xiamen, 361021, China, E-mail: xzhang@iue.ac.cn; Fax: +86-592-6190518; Tel: +86-592-6190519

Table S1. List of chemical reagents.

CAS No	Chemical name	Chemical formula	Molecular characteristic		Manufacturer's name	Supplier
			Weight (g mol^{-1})	Density (g cm^{-3})		
129-00-0	Pyrene	$C_{16}H_{10}$	203.25	1.27	Pyrene	Sigma-Aldrich, USA
2966-50-9	Silver trifluoroacetate	CF_3COOAg	220.88	N/A	Silver trifluoroacetate	Sigma-Aldrich, USA
2923-18-4	Sodium trifluoroacetate	CF_3COONa	136.01	1.49	Sodium trifluoroacetate	Sigma-Aldrich, USA
109-99-9	Tetrahydrofuran	$(CH_2)_3CH_2O$	72.11	0.89	Tetrahydrofuran	Sigma-Aldrich, USA
9003-53-6	Polystyrene	(C_6H_6) n	—	1.05	Polystyrene	Beijing Dk Nano-Technology Co., LTD, China
75-05-8	Acetonitrile	CH_3CN	41.05	0.79	Acetonitrile	Sinopharm Chemical Reagent Co., Ltd (China).
9000-70-8	Gelatin from porcine skin	$C_{102}H_{151}N_{31}O_{39}$	—	1.27	Gelatin	Sigma-Aldrich, USA

Test of normality and homogeneity of variance

Before we perform ANOVA we have done a Shapiro-Wilk's test ($p>0.05$) [1] and a visual inspection of their histograms, normal Q-Q plots and box plots showed that the concentrations were normally distributed for the period of exposure time; with, e.g., intestine, a skewness of 0.60 (SE = 0.712), -0.044 (SE = 0.620), 0.095 (SE = 0.912), and -0.226 (SE = 0.530) for day 1, day 5, day 10, and day 20 respectively and kurtosis of -0.977 (SE = 1.00), -2.179 (SE = 2.30), -2.006 (SE = 2.20), and -1.403 (SE = 2.10) for day 1, day 5, day 10, and day 20 respectively [2,3]. Other examples of the results that were obtained for other tissues such as liver, gill, muscle, and brain were summarized in the table 1. Additionally, a Levene's test verified the equality of variances in the samples (homogeneity of variance) [4].

Zebrafish tissue	Day1				Day 5				Day 10				Day 20			
	Skn	**SE**	**Kts**	**SE**	**Skn**	**SE**	**Kts**	**SE**	**Skn**	**SE**	**Kts**	**SE**	**Skn**	**SE**	**Kts**	**SE**
Intestine	0.60	-0.97	0.71	1.00	-0.04	0.62	-2.17	2.3	0.09	0.9	-2.00	2.20	-0.22	0.53	-1.40	2.10
Liver	0.96	0.75	-0.48	0.64	-0.07	0.89	-2.38	2.00	0.26	0.72	-2.05	2.05	0.15	0.34	1.32	1.65
Gill	0.80	0.91	-0.01	1.23	-2.01	2.15	0.89	0.96	0.13	0.91	-2.17	2.3	0.85	0.97	-1.61	2.10
Muscle	0.75	0.81	-0.65	0.72	1.21	0.98	1.16	2.11	0.80	0.91	0.55	0.74	0.57	0.67	-0.80	1.12
Brain	0.07	0.86	-2.87	2.12	-0.64	0.81	-3.04	2.85	-0.61	0.92	-2.27	2.12	1.41	0.95	1.46	1.67

Table S2. Skewness (Skn) and Kurtosis (Kts) parameters[a]

[a]The abbreviation SE stands for standard error.

Molecular weight distribution of polystyrene nanoplastics as synthetic polymer

Colligative characteristics of polymers, light scattering, and ultracentrifugation, were used to determine molecular weight distribution [5,6]. The arithmetic mean was computed as numerical average by multiplying the molecular weight of each chain M_i by the number of chains of that mass N_i, then adding and dividing by the total number of polymeric chains (eq.1):

$$M_n \frac{N_1M_1 + N_2M_2 + ...N_iM_i}{\sum_i N_i} = \frac{\sum_i N_iM_i}{\sum_i N_i} \quad (1)$$

The number-average molecular weight was calculated as an average molecular weight per molecule because the sum SNiMi can reflect the entire weight of the sample. Analytical techniques such as ebulliometry, cryometry, osmometry, and end-group analysis were used to quantify M_n because the amount of molecules can affect the colligative characteristics of PS polymers [7]. The weight-average molecular weight was determined by multiplying the molecular weight of each chain M_i by its weight Wi, adding them together, and dividing by the total weight of the sample (eq. 2):

$$M_w = \frac{W_1M_1 + W_2M_2 + ...W_iM_i}{\sum_i W_i} = \frac{\sum_i W_iM_i}{\sum_i W_i} \quad (2)$$

A more standard formula (eq. 3) for M_w is derived by replacing $W_i = N_i M_i$:

$$M_w = \frac{\sum_i N_iM_i^2}{\sum_i N_iM_i} \quad (3)$$

The breadth and shape of a polymer's molecular weight distribution (MWD) provided details about its polymerization process and kinetics [8]. The ratio of two molecular weight averages was used to describe the breadth of MWD (eq. 4):

$$PDI = \frac{M_w}{M_n} \quad (4)$$

Where the polydispersity index (PDI) is a ratio that reflects the range of variation in molecular weight distribution. A high polydispersity index (PDI) shows that the sample contains a large number of chains with highly varied molecular weights, while a low polydispersity index

shows that the majority of the molecules in the sample have relatively similar molecular weights [9,10].

Optimization of the sample ratio for PSN analysis with MALDI-TOF-MS

PSN sample was prepared by mixing silver trifluoroacetate, pyrene and polystyrene and the ratio of this mixture was chosen and optimized, where different volumes were varied. The intensities of different mass spectra results were compared one to another to confirm the proper ratio to use for the quantitative analysis of PSN. The mass spectra obtained to investigate PSN with pyrene, and silver trifluoroacetate were not the same especially when there was a change in the volume of the analyte of the cationization reagent. Therefore, the ratio variation and

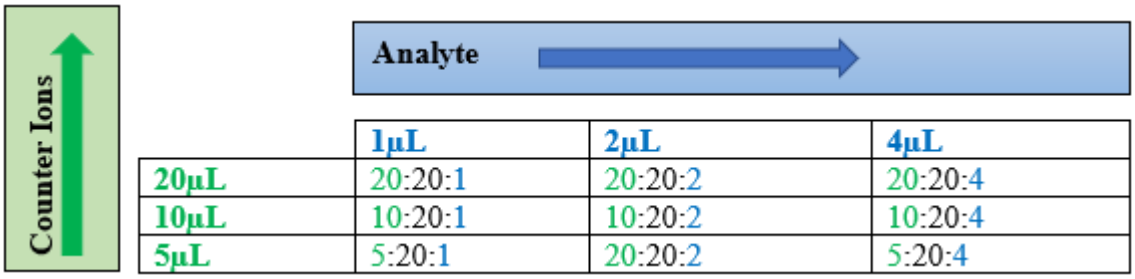

	1µL	2µL	4µL
20µL	20:20:1	20:20:2	20:20:4
10µL	10:20:1	10:20:2	10:20:4
5µL	5:20:1	20:20:2	5:20:4

Fig. S1. Variation of silver trifluoroacetate and polystyrene nanoplastics ratio for optimization

comparison were done to choose the best ratio of the analyte-matrix-cationization agent, that might produce the highest mass spectra, to use for the whole experiment. As show in Figure S1. The solutions were prepared by mixing matrix, analyte and cationization while varying the relative proportions of the components such that nine unique samples mixtures are made. For example, keeping the amount of added pyrene stock solution constant (e.g., 10 µL), vary the amount of PSN solution by a factor of two (e.g., 4, 2, and 1 µL), while also varying the amount of AgTFA solution by a factor of two (e.g., 20, 10, and 5 µL). These samples effectively produced a 3 x 3 grid of samples with the two different concentration variables on the x and y axes. The 3x3 grid for sample ratio determination was done using a 3x3 grid of samples, the relative concentrations of cationization agent-analyte-matrix were systematically varied to empirically determine an optimized sample preparation. This was typically done by holding one of the three variables constant (20 µL of matrix solution) while increasing the amount of the other two (cationization agent (y-axis) and analyte (x-axis) components) by a set multiple (2-fold in the example depicted). As results, the ratio of 5:20:4 (v:v:v) was chosen as the best combination to use for the whole MALDI-TOF-MS quantitative analysis of PSN in the zebrafish tissues.

Effect of the matrix and cationization reagent concentration on peak intensity in MALDI-TOF-MS analysis

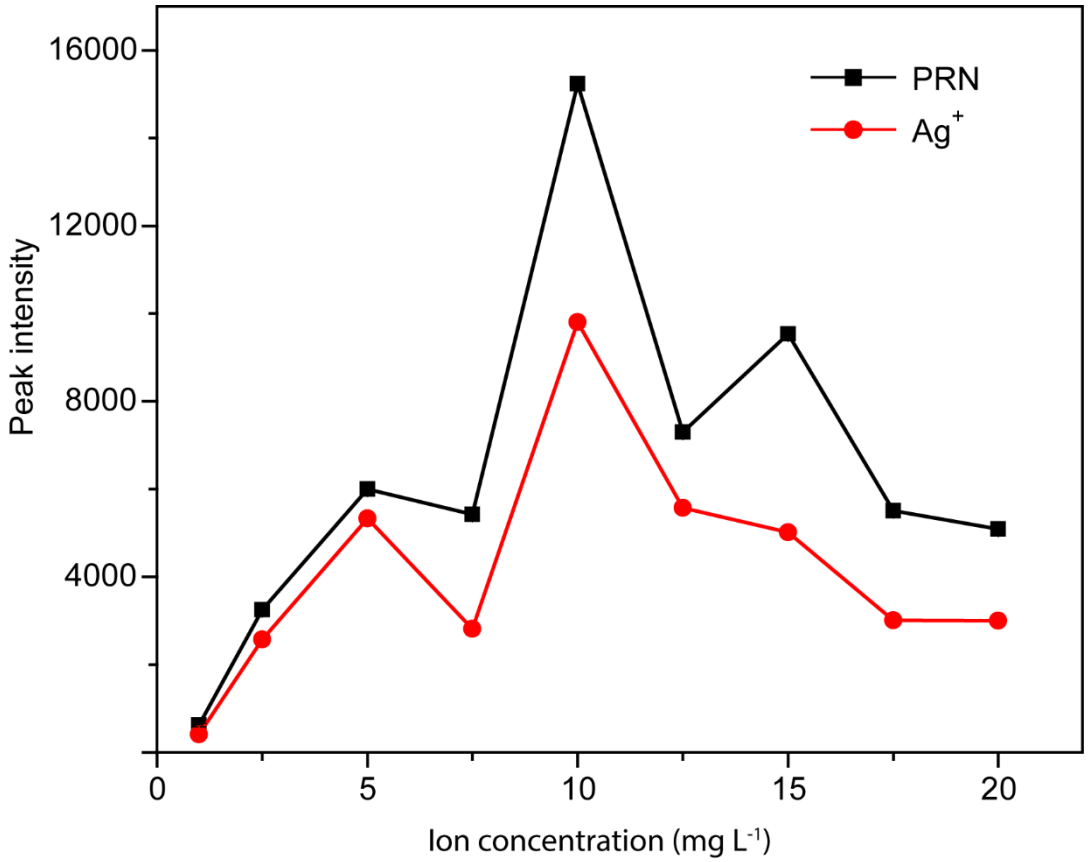

Fig. S2. The effect of matrix (pyrene abbreviated as PRN) and cationization reagent concentration (AgTFA) on peak intensity in MALDI-TOF-MS analysis.

A series of experiments were done to choose the concentration that had the highest peak intensity particularly when the mixture of pyrene (PRN) and silver trifluoroacetate (AgTFA) were made at a ratio of 5:20 (v/v). Therefore, the concentration of 10 mg L-1 was chosen for both matrix and cationization reagent. At this concentration there was a highest peak intensity of more than 14600. The other concentrations were ignored and 10 mg L-1 was used in all experiment of real sample detection of MALDI-TOF-MS analysis of polystyrene nanoplastics polymer. Therefore, the ratio of 5:20:4 (v/v/v) was used, for the standards, in the detection of PSN polymers in zebrafish samples.

Impact of the matrix-type in the MALDI-TOF-MS analysis of PSN

In-depth comparison between conventionally used matrices, polar matrices, and nonpolar matrices has been made. The comparison has revealed that the combination of polar matrices such as 2,5-dihydroxybenzoic acid (DHB), dithranol (DI), 2-(4-hydroxyphenylazo) benzoic acid (HABA), sinapic acid (SA) and trans-3-indoleacrylic acid (IAA) with silver cationization reagent, e.g., Ag (CF3COO) (silver trifluoroacetate: AgTFA) and other silver related-salts bring silver cluster ions on the MALDI-TOF-MS analysis of polystyrene nanoplastic polymers [11]. In contrast, it was previously reported that the combination of nonpolar matrices, namely pyrene (PRN), anthracene (ATH) and acenaphthene (ACTH) do not generate silver cluster ions on the MALDI-TOF-MS analysis and PRN was found to serve as the best matrix among the nonpolar matrices [11]. Therefore, during the detection of PSN in different tissues of zebrafish, pyrene was selected and used as a nonpolar matrix to avoid the interference of silver cluster ions in the results.

In this respect, a series of experiments were conducted to choose the proper concentration during the analysis of the analyte (PSN). The optimal conditions, particularly for the mixture of PRN and AgTFA, were found at a ratio of 20:5 (v/v). Therefore, the concentration of 10 mg L^{-1} was chosen for both the matrix and cationization reagent as shown in Fig. S2. MALDI-TOF-MS results presented in Fig. S3 confirmed the presence of PSN in different endpoints of zebrafish tissues without silver cluster interferences. Therefore, it is suggested that the combination of a nonpolar matrix, PRN, and AgTFA to investigate nonpolar polymers (e.g., PSN) should be a promising choice and approach to use in MALDI-TOF-MS analysis of nanoplastics, particularly, in animal tissues in the future of nanotechnology-research works.

Exposure of zebrafish tissues at different concentration of PSN

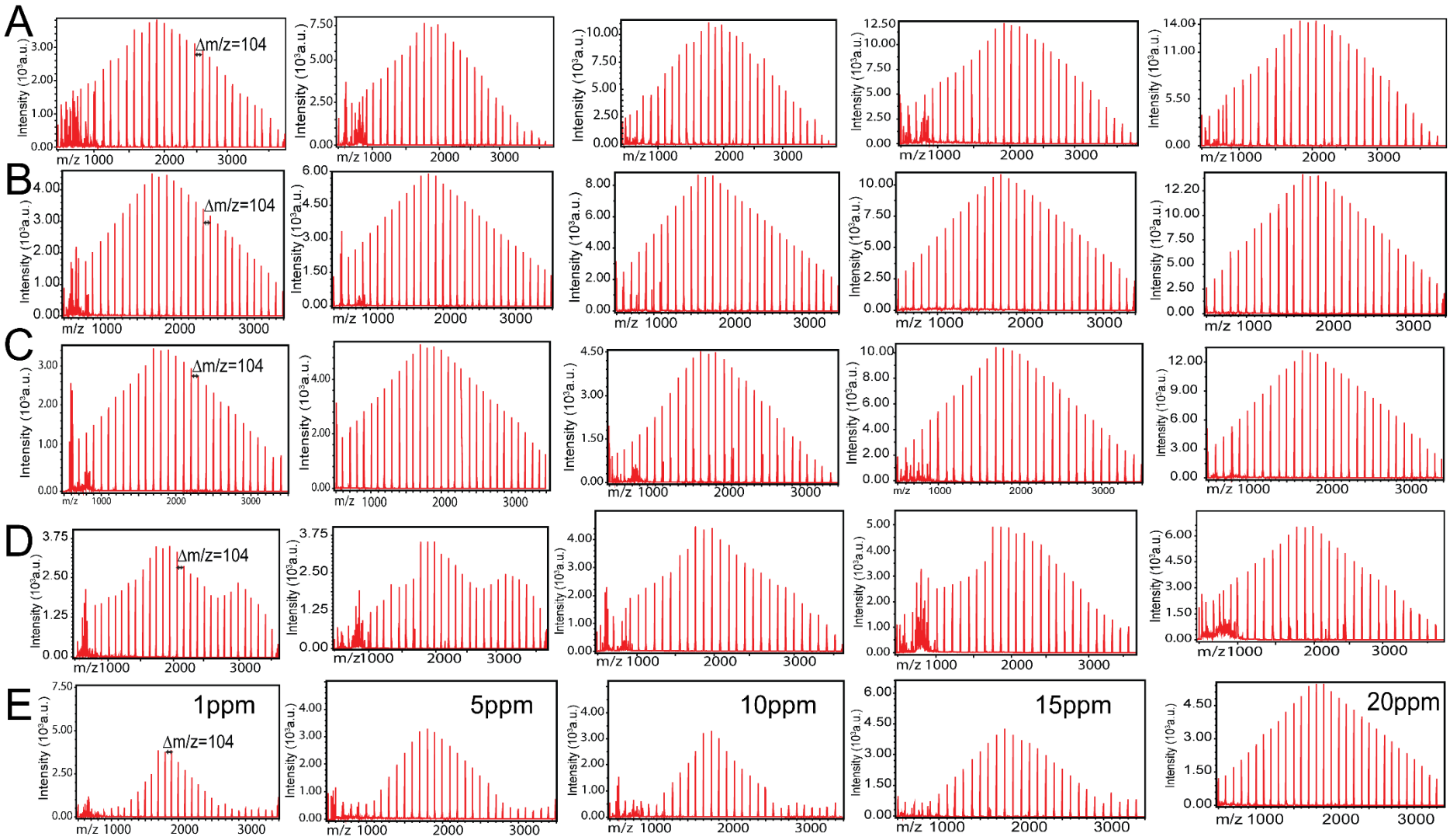

Fig. S3. MALDI-TOF-MS positive reflection mode mass spectra of PSN detected in A: intestines, B: livers, C: gills, D: muscles, and E: brain, Each and every zebrafish tissue was exposed to five different concentrations (1, 5, 10, 15, and 20 ppm) for 20 days.

Sample preparation and quantification of PSN with MALDI-TOF-MS

During quantification analysis, exposed and control zebrafish were euthanized in ice water (0–4 ^{o}C) for at least 10 min and then washed with deionized water to avoid the sample contamination. Fresh tissues such as the intestine, liver, gill, muscle and brain, that were originally exposed to five different concentrations of PSN (1, 5, 10, 15, and 20 mg L^{-1}), were dissected. For each type of tissue, in order to get enough tissue samples, five fish were randomly selected from each group of concentration to collect target tissues. Homogenization, for each type of tissue, was carried out follows: Tissues (each type of tissues such as intestine, liver, gill, muscle, and brain), were homogenized using automated grinding device, TissueLyser (Qiagen) and FastPrep-24 (MP Biomedicals, Santa Ana, CA, U.S.A.) with a pinch of glass powder [(the mean ± standard deviation (SD): 86.60± 5.81), (Glass beads, ref. G4649-500G; Sigma-Aldrich, St. Louis, MI, U.S.A.) as a disruptor. The settings selected the homogenizer device were identical to those previously established as optimal for the other animal tissues [12]. These parameters were 3 cycles of 60 s at a frequency of 30Hz with the TissueLyser machine (condition 1), and 4 cycles of 40 s at a frequency of 6 movements per second (m/s) with the FastPrep-24 apparatus (condition 2). Grinding by pestle was kept as the reference method. For all the conditions tested, optimized volumes of supply buffers for each species were used [13]. A mix of 20 µL of 70% formic acid (v/v) (Sigma) plus 20 µL of 50% acetonitrile (v/v) (Fluka, Buchs, Switzerland) was used. The settings for the instrument were then applied to homogenize the samples from tissues stored under the conditions selected. Therefore, the supernatant from each sample, pyrene matrix and silver trifluoroacetate as cationization reagent were combined at a ratio of 4:20:5 (v/v/v) respectively. 1µL of the the combined solution was deposited on the MALDI-TOF target plate for quantitative analysis. An Autoflex III MALDI-TOF mass spectrometer (Bruker Daltonics, Bremen, Germany) equipped with a laser working at a wavelength of 377 nm was used to acquire all mass spectra. The negative ion linear mode was firstly used for the analysis of polystyrene nanoplatics. In these experiments there was no response observed in the mass spectra that were obtained. Therefore, the positive ion linear mode was employed to record the spectra. In this case there were the abundant PSN responses in all mass spectrums of different samples. For the MS tests, a standard MTP384 polished steel target (Bruker Daltonics) was utilized. For each range, five pulses at 100 distinct locations were collected (representing one pixel). The FlexAnalysis software version 3.4 (Bruker Daltonics) was used to analyze the data. During the analysis of polystyrene nanoplastics, it was observed that the increase of the response (intensity, a.u.) of

the PSN standards was proportional to the augmentation of concentration of the analyte. Therefore, the calibration curve was established between the concentrations and the intensities to determine the accumulated concentration in the zebrafish. Meanwhile, we have carried out a series of experiments to confirm whether the optimal conditions of quantification methods could be used determine the amount of polystyrene nanoplastics accumulated in the tissue of zebrafish. In this respect, spiked zebrafish samples were prepared where zebrafish tissues were injected the known concentrations (1, 5, 10, 15, 20 mg L^{-1}) so that the established linear relationship could be verified over theses samples. The established standard curve was confirmed to be used on the real samples as long as the recoveries, for the determination of polystyrene nanoplastics in different spiked zebrafish tissues (intestine, liver, gill, muscle, and brain), was ranging 98.8-105.6 % in all investigated zebrafish tissues. These results gave the green light on the analysis of PSN in the real samples using the originally established standard curve for the experimentally exposed zebrafish (Danio Rerio).

Enrichment ability of PSN in different tissues of zebrafish

The experimental results revealed that during the exposure time period of 20 days the high concentration of PSN accumulated first of all in the intestine followed by liver, gill, muscle and brain. This means that the amount of PSN detected, on each sampling time slot, in different tissues was higher particularly in the intestine but the muscle and brain collected the lowest amount of PSN as shown in different sections of this work. Therefore, even if there was a variation of the uptake rate of PSN in various tissues, PSN might accumulate in the intestine, liver and gill faster than in the muscle and brain and this was probably linked to the exposure pathways of the plastic nanoparticles as it was previously reported [14–16]. The results showed that both muscle and brain collected limited amount of PSN, compared to the other tissues. Thus, this shows that even though the plastic nanoparticles have entered the circulatory system, but there was not high concentration of PSN to accumulate in the muscle probably because of the characteristics of PSN and the muscle itself. On the other hand, the PSN might not easily passed the blood-brain barrier, and resulted in the lowest uptake rate of PSN in the brain organ. Consequently, it was reasonable for the result of the small amount of PSN detected in this organ during the uptake period.

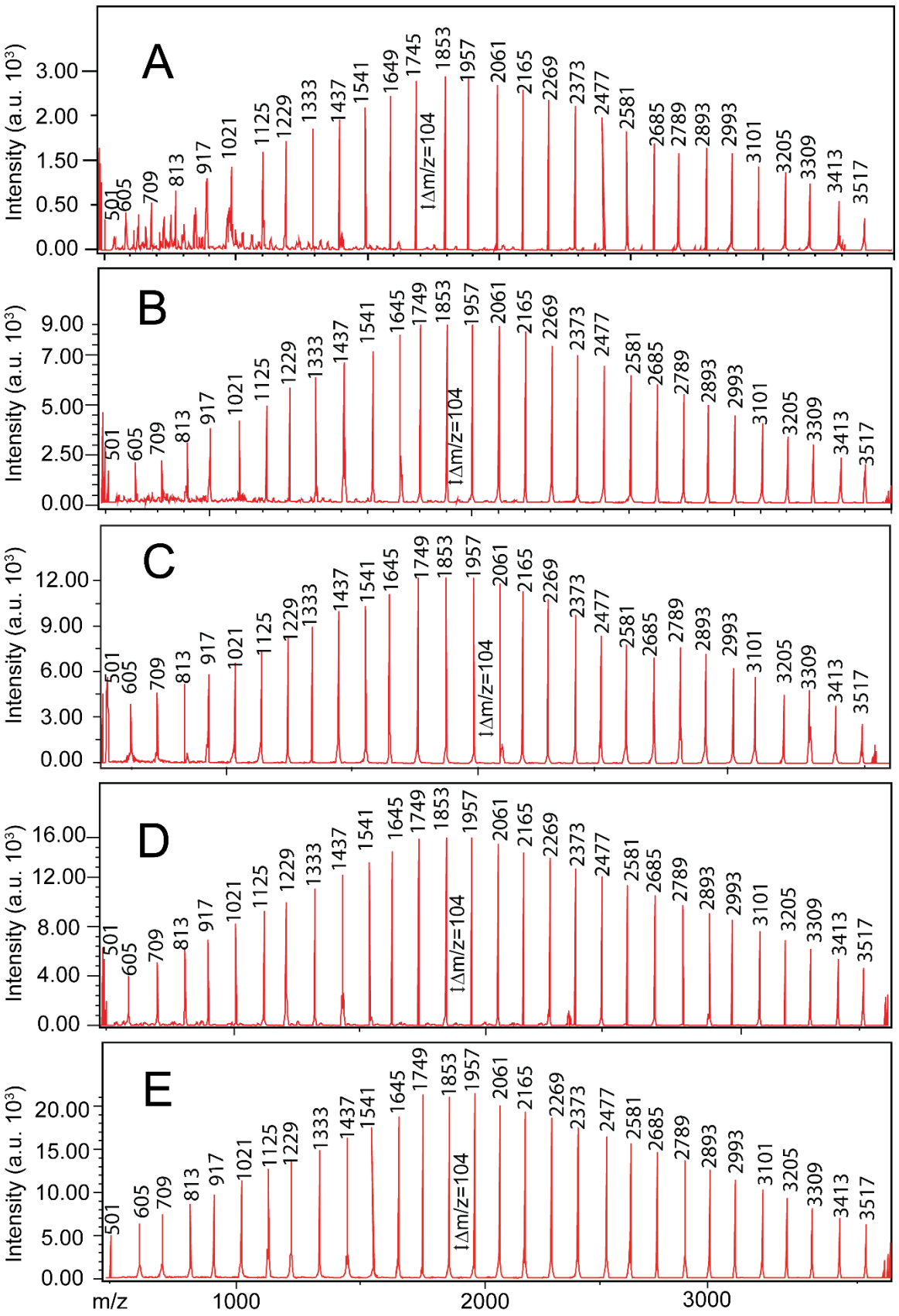

Fig. S4. MALDI-TOF-MS positive reflection mode mass spectra of PSN standards detected at different concentration; A: 0.4 mg L^{-1}, B: 5 mg L^{-1}, C: 10 mg L^{-1}, D: 15 mg L^{-1}, and E: 22 mg L^{-1}.

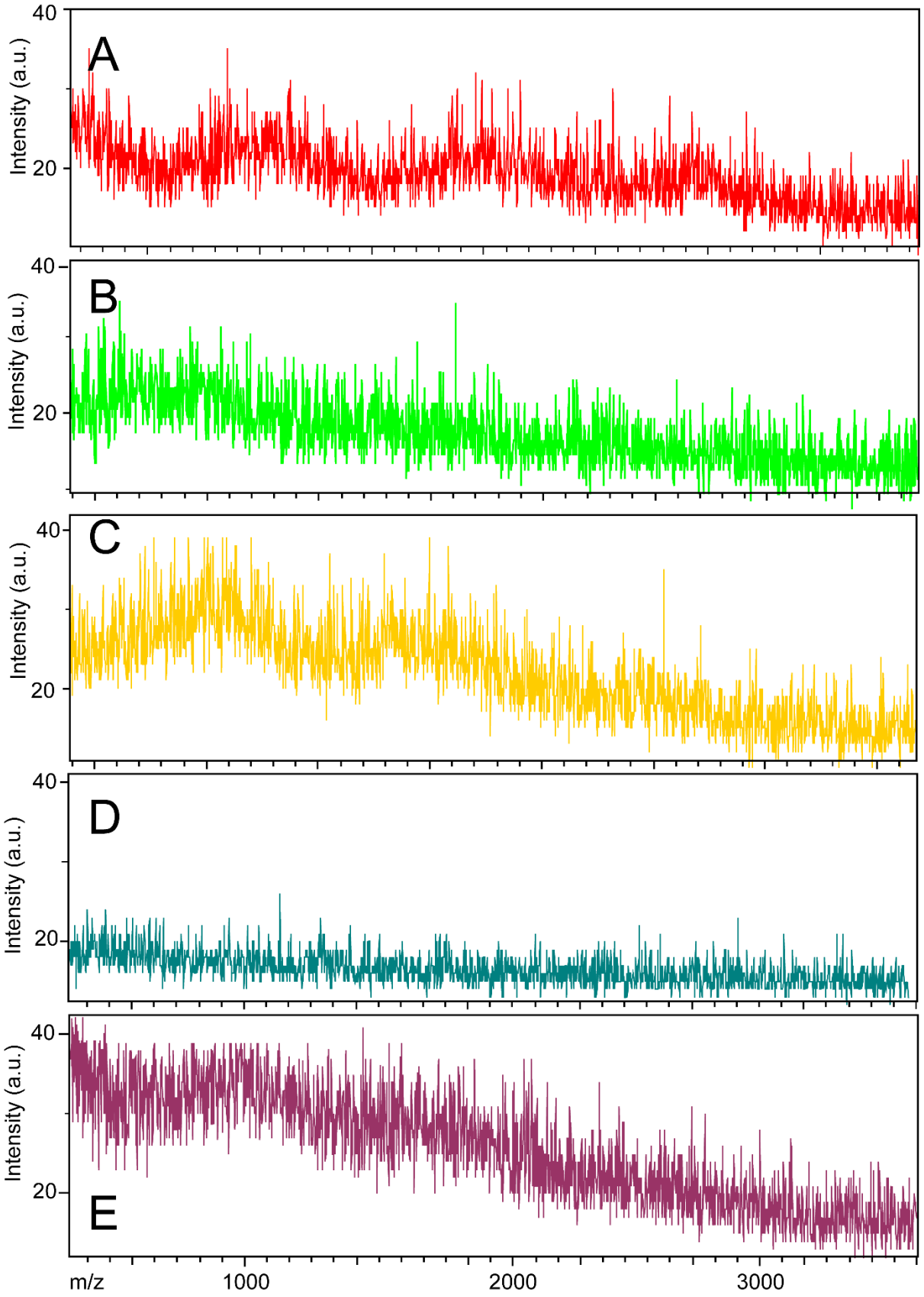

Fig. S5. MALDI-TOF-MS positive reflection mode mass spectra of obtained in the control zebrafish tissues: A: intestine, B: liver, C: gill, D: muscle, and E: brain.

Reference

1 S.S. Shapiro, and M.B. Wilk, An Analysis of Variance Test for Normality (Complete Samples), *Biometrika*., 1965, **52**, 591.

2 Y. Bee Wah, and N. Mohd Razali, Power comparisons of Shapiro-Wilk, Kolmogorov-Smirnov, Lilliefors and Anderson-Darling tests, *J. Stat. Model. Anal.*, 2011, **2**, 21–33.

3 D. Cramer, and D. Howitt, The SAGE Dictionary of Statistics, *SAGE Dict. Stat.*, 2011, .

4 W.E. Martin, and K.D. Bridgmon, Quantitative and statistical research methods From hypothesis to results.

5 W.-F. Su, Polymer size and polymer solutions, in: Princ. Polym. Des. Synth., Springer, : pp. 9–269–26.

6 M. Wagner, C. Pietsch, L. Tauhardt, A. Schallon, and U.S. Schubert, Characterization of cationic polymers by asymmetric flow field-flow fractionation and multi-angle light scattering—a comparison with traditional techniques, *J. Chromatogr. A*., 2014, **1325**, 195–203.

7 J.W.A. van den Berg, and J. Schuijer, Molecular Structure Determination and Characterization, in: Macromol. Biomater., CRC Press, : pp. 19–5619–56.

8 G. Capaccio, and I.M. Ward, Preparation of ultra-high modulus linear polyethylenes; effect of molecular weight and molecular weight distribution on drawing behaviour and mechanical properties, *Polymer (Guildf).*, 2015, **15**, 233–238.

9 N. Ghahramani, and M. Rahmati, The effect of the molecular weight and polydispersity index on the thermal conductivity of Polyamide 6: A molecular dynamics study, *Int. J. Heat Mass Transf.*, 2020, **154**, 119487.

10 Y. Guillaneuf, and P. Castignolles, Using apparent molecular weight from SEC in controlled/living polymerization and kinetics of polymerization, *J. Polym. Sci. Part A Polym. Chem.*, 2008, **46**, 897–911.

11 T. Habumugisha, Z. Zhang, J.C. Ndayishimiye, F. Nkinahamira, A. Kayiranga, E. Cyubahiro, A. Rehman, C. Yan, and X. Zhang, Evaluation and optimization of the influence of silver cluster ions on the MALDI-TOF-MS analysis of polystyrene

nanoplastic polymers, *Anal. Methods*., 2022, **14**, 763–772.

12 N. Bydlinski, Www.proteomics-journal.com Page 1 Proteomics, *Proteomics*., 2016, 1–25.

13 A. Yssouf, C. Socolovschi, C. Flaudrops, M.O. Ndiath, S. Sougoufara, J.S. Dehecq, G. Lacour, J.M. Berenger, C.S. Sokhna, D. Raoult, and P. Parola, Matrix-Assisted Laser Desorption Ionization - Time of Flight Mass Spectrometry: An Emerging Tool for the Rapid Identification of Mosquito Vectors, *PLoS One*., 2013, **8**, 1–10.

14 W. Huang, B. Song, J. Liang, Q. Niu, G. Zeng, M. Shen, J. Deng, Y. Luo, X. Wen, and Y. Zhang, Microplastics and associated contaminants in the aquatic environment: A review on their ecotoxicological effects, trophic transfer, and potential impacts to human health, *J. Hazard. Mater.*, 2021, **405**, 124187.

15 J.F. Provencher, J. Ammendolia, C.M. Rochman, and M.L. Mallory, Assessing plastic debris in aquatic food webs: what we know and don't know about uptake and trophic transfer, *Environ. Rev.*, 2019, **27**, 304–317.

16 M. Bergmann, L. Gutow, and M. Klages, Marine anthropogenic litter, *Mar. Anthropog. Litter*., 2015, 1–447.